



Application of a Taguchi L_{16} orthogonal array for optimizing the removal of Acid Orange 8 using carbon with a low specific surface area

M.P. Elizalde-González*, L.E. García-Díaz

Centro de Química, Instituto de Ciencias, Universidad Autónoma de Puebla, Edificio 103 H, C.U. Col. San Manuel, Puebla, Pue. C.P. 72570, Mexico

ARTICLE INFO

Article history:

Received 16 April 2010

Received in revised form 14 July 2010

Accepted 19 July 2010

Keywords:

Taguchi method

Optimization

Carbon

Guava seeds

Acid Orange 8

Adsorption

ABSTRACT

The conditions for the adsorption of the dye Acid Orange 8 onto carbon were optimized using the Taguchi method. Four samples of activated carbon were obtained from guava seeds, and their textures were characterized by nitrogen adsorption isotherms. The equilibrium adsorption isotherm on mesoporous carbon ($114 \text{ m}^2 \text{ g}^{-1}$) showed multilayer adsorption behavior with a kinetic curve that could be described by the Ho equation. To achieve maximum dye removal, the effects of temperature ($10\text{--}40^\circ\text{C}$), specific surface area ($67\text{--}143 \text{ m}^2 \text{ g}^{-1}$), initial concentration ($250\text{--}1500 \text{ mg L}^{-1}$), pH ($2\text{--}13$), and the mass–volume ratio ($10\text{--}150 \text{ g L}^{-1}$) were studied using an L_{16} orthogonal array. The percent dye removal was transformed into an accurate S/N ratio for a “high is better” response. pH was found to be the most effective factor for promoting dye removal, followed by the mass–volume ratio. A temperature of 10°C , a specific surface area of $114 \text{ m}^2 \text{ g}^{-1}$, an initial concentration of 500 mg L^{-1} , pH 2, and a mass/volume ratio of 150 g L^{-1} were the best conditions determined by the Taguchi method. Finally, the carbon was tested using samples of real and simulated wastewater solutions under the optimal conditions, and color removal efficiencies of 60% and 40%, respectively, were obtained.

© 2010 Elsevier B.V. All rights reserved.

1. Introduction

The textile industry uses water as the main medium for applying dyes and removing impurities. Major concerns arise from these methods, for example the quantity of water necessary for processing, the quality of the water discharged, and the chemical load introduced by the process pollutants [1]. Acid Orange 8 (AO8) belongs to the azo dye family, which accounts for over 50% of the world's annual production of one million tons of dye [2]. The adsorption of AO8 by carbonaceous materials has not been widely reported [3–6]. In contrast, Acid Orange 7 (AO7), which differs from AO8 by only one methyl group, is one of the most studied [7] aryl azo naphthol dyes. These dyes normally exist in their hydrazone tautomeric forms, which exhibit good stability. In this form, they are resistant to photo-oxidation and chemical oxidation. The aromatic amines are the principal products of cleavage of the azo group, and these are potentially mutagenic and carcinogenic [8]. However, the toxicity of AO8 has not been reported.

In general, polar hydrophilic environmental pollutants are readily soluble in water and are, therefore, difficult to remove during water treatment processes. AO8 is an important commercial tex-

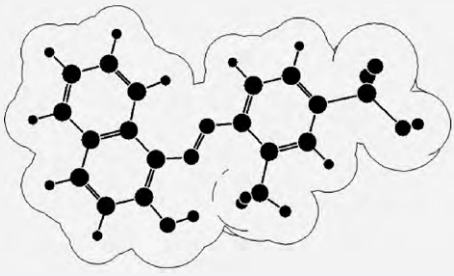
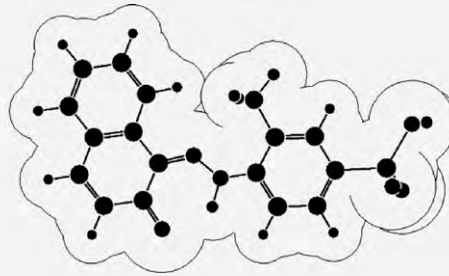
tile dye. As a strong electrolyte, it is completely dissociated under the acid conditions used in the dyeing process. Its principal application is in leather dyeing and paper coloration, and the second principal application is in wool dyeing, which makes its waste by-products an important economic regional issue. AO8 possesses no outstanding coloristic properties among the acid monoazo dyes, but it is distinguished by the brilliance of its shade and particularly low production cost. Anionic monoazo dyes are still used in larger quantities for cheap articles and, consequently, are abundant in wastewater [9]. Typical textile wastewater is composed, for example, of 5% anionic dyes [10]. AO8 was one of the 10 detected dyes in water samples from municipal and industrial wastewater treatment plants in Northern Italy in 2002, together with phenols, carboxylic acids, aromatic sulfonates, aromatic amines, pharmaceuticals and surfactants [11].

The removal of dyes without producing secondary degradation products is an important advantage of the adsorption process [12]. Dye removal depends on several factors that relate narrowly to the adsorption experimental conditions and to the adsorbent characteristics. The prevailing view is that the magnitude of the specific surface area plays a major role in adsorption. The system parameters have been investigated to establish the optimal conditions for dye removal. Optimization methods, such as the response surface [13] and the Taguchi technique [14], have been used to achieve the best response under the given removal conditions. Elizalde-González and Hernández-Montoya [7] reported an optimization

* Corresponding author. Tel.: +52 222 2295500; fax: +52 222 2295525.

E-mail addresses: melizald@siu.buap.mx, maria.elizalde.uap.mx@gmail.com (M.P. Elizalde-González).

Table 1
Principal characteristics of the tautomeric forms of the dye Acid Orange 8.

Characteristic	Azo form	Hydrazone form
CI 15575		
CAS 5850-86-2 ~65% purity		
Formula $C_{17}H_{13}N_2NaO_4S$		
Molecular weight ($g\ mol^{-1}$) 342.37		
		
	↔	
Natural pH in deionised water	7.1	
Molar volume ($cm^3\ mol^{-1}$)	224.2	232.7
Name	3-Methyl-4-(2 hydroxi-1-naphthylazo) benzenesul-fonic acid sodium salt	3-Methyl-4-[N'-(2-oxo-2H-naphthalen-1-ylidene)-hydrazino]-benzenesul-fonic acid sodium salt
Molecular volume (nm^3)	0.281	0.280
Molecular surface area (nm^2)	3.33	3.32
Molecular dimensions (nm)	Length 1.58; width 1.03; depth 0.54	Length 1.64; width 0.96; depth 0.54
Calculated pK_a	$pK_1 -1.0 \pm 0.5$; $pK_2 13.5 \pm 0.5$	$pK_1 -0.2 \pm 0.5$; $pK_2 9.4 \pm 0.2$

study using the Taguchi method with consideration for the factors that affect dye removal. The Taguchi technique includes the design of an experiment process that uses orthogonal arrays that allow for the independent evaluation of factors through a small number of trials [15]. This technique includes data transformation to a signal-to-noise (S/N) ratio, which is a measure of the variations presented.

Nowadays, a variety of carbonaceous adsorbents are available from the pyrolysis of lignocellulosic materials and agricultural wastes, such as fruit seeds [16]. These materials have been widely tested for removing pollutants from aqueous solutions. A variety of commercial carbons exist, and no single value has been established to determine if a carbon has a small or large specific surface area. Activated carbon cloths have a high specific surface area of $1500\ m^2\ g^{-1}$, and the main advantage is a faster adsorption rate relative to that of activated carbon [3]. Lignin-cellulose precursors, for example, avocado fruit peel [17] yield low specific surface areas, considered $<2\ m^2\ g^{-1}$ in [18].

Previous results have shown that mesoporous carbon obtained from guava seeds adsorb larger quantities of AO8 than of AO7 [6] under the same conditions. Contradicting results were obtained from measurements of the adsorption by microporous carbon obtained from mango seeds [5] or from mesoporous activated carbon cloth [4]. AO8 yielded greater kinetic adsorption coefficients [3] but smaller ultrasonic degradation rates [19] than AO7.

In the present work, we prepared a set of samples of activated carbon from guava seeds (*psidium guajava*)—a waste material from juice factories—and used the Taguchi method to examine the influence of other system factors on the removal of AO8 on the prepared activated carbon substrates with low specific surface areas. UV-visible spectra were examined previously to evaluate the effects on the adsorption measurements, because AO8 tends to aggregate and form azo-hydrazone tautomers [20]. Finally, the carbon was assayed using a sample of wastewater from a textile factory as well as an artificial wastewater prepared in the laboratory.

2. Materials and methods

2.1. Precursor and preparation of carbon

The guava seeds were obtained from fresh fruit coming from Aguascalientes, Mexico. The seeds were washed with deionized water and dried at room temperature for 48 h. To obtain 1.00 and 1.19 mm particles, the seeds were ground and sieved. Finally, they were used as raw materials for obtaining carbon using a horizontal tubular CARBOLITE furnace with a EURO THERM controller under atmospheric conditions. Two heating programs with final temperatures of 500 or 600 °C were used. The temperature programs comprised two heating ramps: the first ramp began at room temperature and increased to 70 °C at a rate of $8\ ^\circ C\ min^{-1}$, and the second ramp began at 70 °C and increased to a final temperature at a rate of $5\ ^\circ C\ min^{-1}$, followed by 4 h isothermal heating. Finally, the carbon samples were ground, sieved, and analyzed to obtain their textural characteristics.

2.2. Adsorption experiments

Adsorption tests were conducted in static batch experiments using polycarbonate cylindrical cells with a lid. The kinetic study was carried out under the following conditions: a temperature of 20 °C, an initial concentration of $100\ mg\ L^{-1}$, and a mass-volume ratio of $33\ g\ L^{-1}$. The adsorption isotherm was obtained at the same temperature and with the same mass-volume ratio. The initial concentrations ranged from 50 to $3000\ mg\ L^{-1}$, and the contact time was 24 h. Finally, the quantity of adsorbed dye was calculated using the relation: $a = (C_i - C_f)V/m$, where a ($mg\ g^{-1}$) represents the amount of dye adsorbed, C_i ($mg\ L^{-1}$) is the initial dye concentration, C_f is the final equilibrium concentration ($mg\ L^{-1}$), V is the solution volume in the cell (L), and m is the weight of the adsorbent (g). We presumed that electrolytes and dyeing additives in the commercial dye could generate multi-solute adsorption, but we assumed that the UV-vis adsorption measurements corresponded to the adsorption of single dye molecules.

Table 2
Experimental L_{16} orthogonal array and results of the removed dye in two independent experiments.

Experiment	Factor levels					Removed dye (%)		(S/N) _{HB}
	A	B	C	D	E	Experiment 1	Experiment 2	
1	1	1	1	1	1	8.9	7.8	18.36
2	1	2	2	2	2	5.0	5.47	14.28
3	1	3	3	3	3	6.5	7.2	16.70
4	1	4	4	4	4	7.2	6.9	16.97
5	2	1	2	3	4	7.1	6.4	16.59
6	2	2	1	4	3	4.3	4.4	12.77
7	2	3	4	1	2	19.2	22.5	26.29
8	2	4	3	2	1	1.5	1.5	3.60
9	3	1	3	4	2	3.1	3.5	10.33
10	3	2	4	3	1	1.1	1.5	1.98
11	3	3	1	2	4	16.4	14.1	23.58
12	3	4	2	1	3	23.9	24.7	27.71
13	4	1	4	2	3	3.6	2.8	10.01
14	4	2	3	1	4	77.0	74.8	37.60
15	4	3	2	4	1	4.2	5.2	13.21
16	4	4	1	3	2	0.6	0.9	-3.30

2.3. Optimization of the adsorption conditions

The AO8 dye (Aldrich) and its characteristics are given in Table 1. The concentration of ions determined by ion chromatography was 8.3 mg L^{-1} chloride and 0.6 mg L^{-1} sulfate. An experimental L_{16} array from the Taguchi method was applied for the optimization of the adsorption conditions. The five factors selected were: temperature (10, 20, 30, 40°C), specific surface area (67, 89, 114, $143 \text{ m}^2 \text{ g}^{-1}$), initial concentration (250, 500, 1000, 1500), pH (2, 6, 10, 13), and mass–volume ratio (10, 50, 100, 150 mL^{-1}). The array of the experimental factors and the levels are given in Table 2. The pH was adjusted using NaOH and HCl solutions. The solution was separated from the adsorbent by filtration after 24 h equilibrium. Mixed cellulose ester membrane disk filters ($0.45 \mu\text{m}$ pore size) did not produce any variations in the absorbance before or after filtration. The adsorption solutions were subsequently centrifuged ($12,000 \text{ rpm}$) to measure the final dye concentration.

Taguchi created an experimental data transformation, which is a measure of the response variations that are present. The transformation is the signal-to-noise (S/N) ratio, which depends on the characteristic measured. The “higher is better” (HB) ratio:

$$(S/N)_{HB} = -10 \log(1/r \sum_{i=1}^r 1/y_i^2), \text{ where } y_i \text{ is the experimental response and } r \text{ is the number of test in the trial, was used because}$$

a high rate of dye removal was desirable.

The molecular volume, area, and dimensions were calculated using the software Physical Properties Pro from Chem SW after energy minimization. Calculations of the pK_a were performed using the Software pK_a DB from ACD Inc. In the computation, the dye salt

Table 3
Textural and chemical characteristics of the carbon samples used in the optimization experiments.

Carbon sample	SG-20	SG-23	SG-26	SG-30
Carbonization temperature ($^\circ\text{C}$)	500	500	500	600
Particle size (μm)	500	595	707	841
S_{BET} ($\text{m}^2 \text{ g}^{-1}$)	109	66	204	143
S_{III} ($\text{m}^2 \text{ g}^{-1}$)	89	67	114	143
ΔS_{spe} ($\text{m}^2 \text{ g}^{-1}$)	20	1	90	–
C value	0.51	1.13	0.24	–
$(p/p_0)_m$	0.58	0.48	0.67	–
a_m ($\text{cm}^3 \text{ g}^{-1}$)	20	15	26	–
\bar{D}_p (nm)	5.3	7.6	4.0	4.8
V_{Total} ($\text{cm}^3 \text{ g}^{-1}$)	0.090	0.090	0.089	0.155
Acidity ($\mu\text{mol m}^{-2}$)	9.1	11.1	8.1	6.2
Basicity ($\mu\text{mol m}^{-2}$)	8.1	8.8	7.3	5.5
pH_{pzc}	6.2	5.4	7.1	7.3

D-SO₃Na was considered to be present in its hydrogenated form, D-SO₃H. Intermolecular hydrogen bonding was not considered.

2.4. Real and simulated textile wastewater

The real wastewater was collected from a local textile mill. The sample was taken at the end of a dyeing bath process prior to any treatment; it was allowed to sediment, and the clarified mixture was separated for use in the adsorption experiments. Simulated wastewater was prepared using NaCl (70 g L^{-1}), Na₂CO₃ (5 g L^{-1}), NaOH (4 g L^{-1}), AO8 (10 mg L^{-1}), Carmine Red (15 mg L^{-1}), and Basic Blue (7 mg L^{-1}). Both wastewater samples were characterized, and the adsorption experiments were carried out. The percent of color removal was determined by measuring the absorbance at 436, 525 and 620 nm according to the German ordinance for the discharge of textile wastewater [10,21], and the color intensity was calculated using the following ratio: color (absorbance, m^{-1}) = absorbance \times dilution factor/path length (m) [22].

2.5. Analytical methods

2.5.1. Carbon characterization

The carbon samples were analyzed by measuring the N₂ adsorption isotherms using an automated adsorption apparatus Quantachrome/Autosorb-1. The specific surface area was calculated using the Brunauer–Emmett–Teller (BET) equation, and a correction was applied according to the validity of the BET procedure for type III isotherms (IUPAC) [23]. The pore size distribution was calculated using the Barret–Joyner–Halenda (BJH) equation. In addition, the acidity, basicity, and point of zero charge of the carbon samples were determined by potentiometric titration according to the reported methodology [24] using 0.1 N NaOH, 0.1 N HCl, and a Metrohm–Titrand apparatus.

2.5.2. Dye removal measurement

The dye removal was monitored using a HACH DR5000 spectrophotometer at 490 nm, the dominant wavelength for the AO8. Solutions of AO8 with concentrations 250, 500, 1000, and 1500 mg L^{-1} at pH 2, 6, 10, and 13 were prepared. The effect of pH on the spectrophotometric measurements was examined by calibrating each solution. The percent dye removal was calculated using the equation: $r(\%) = (C_i - C_f)(100/C_i)$, where r represents the percent of removal, and C_i and C_f are the initial and final concentrations (mg L^{-1}). An analogous formula was used for the removal of color, total suspended solids (TSS), nitrates, sulfates, total organic carbon (TOC), and chemical oxygen demand (COD) of the wastewa-

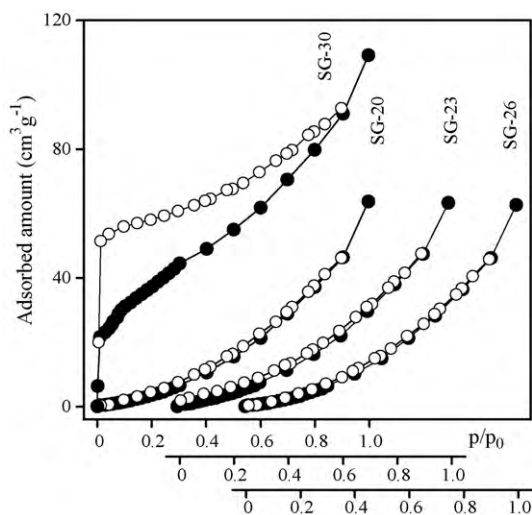


Fig. 1. Adsorption isotherms of nitrogen at $-196\text{ }^{\circ}\text{C}$ on the carbon samples: SG-20, SG-23, SG-26 (type III isotherms) and SG-30 (type II). Full symbols indicate adsorption, hollow symbols indicate desorption.

ter samples. The parameters listed above were quantified using the standard protocols associated with the HACH spectrophotometer.

3. Results and discussion

3.1. Activated carbon

Four samples of carbon were selected after the nitrogen adsorption analysis. Their textural and chemical characteristics are shown in Table 3, where \bar{D}_p is the average pore diameter and V_{Total} is the total volume of the N_2 adsorbed. The samples SG-20, SG-23, and SG-26 were carbonized at $500\text{ }^{\circ}\text{C}$, and the adsorption isotherms obtained were type III, according with the IUPAC classification (Fig. 1). This type of isotherm is displayed by nonporous or macroporous solids. Type III isotherms result if the value of C is less than 2 (Table 3) and the inflection point is barely visible. In such cases, it may be necessary to correct the specific surface area calculated by the BET equation: $1/a(p/p_0 - 1) = (1/a_m C) + (C - 1/a_m C)p/p_0$, where (p/p_0) is the relative pressure, a is the quantity adsorbed,

a_m is the quantity adsorbed on the monolayer, and C is the constant of adsorption. A plot of $1/a(p/p_0 - 1)$ versus (p/p_0) yields a straight line, usually in the range $0.05 \leq p/p_0 \leq 0.35$. The constant C and a_m may be calculated from the slope and the intercept of the BET plot. The total surface area may be calculated using $S_t = (a_m/22,414) \cdot W \cdot A \cdot 10^{-20}$, where W is the adsorbate molecular weight (N_2) and A is Avogadro's number [25]. The correction consists of locating the "BET monolayer point" using the monolayer relative pressure $(p/p_0)_m$ at which the quantity adsorbed is the monolayer capacity a_m [23]. First, C of the BET equation is calculated from the experimental isotherm in the relative pressure range of 0.05–0.35. Once C is known, the monolayer point is calculated using the relation $(p/p_0)_m = (-1 \pm C^{-1/2})/(C - 1)$. With the $(p/p_0)_m$ value, it is possible to determine the quantity adsorbed in the monolayer (a_m) by interpolation of the experimental isotherm data set. By dividing S_t by the sample weight, one can calculate S_{BET} or S_{III} , depending on the procedure used to obtain a_m , i.e., the BET plot for the type II isotherm or isotherm interpolation due to the correction for the type III isotherms.

Table 3 shows the difference (ΔS_{spe}) between S_{BET} and S_{III} . Occasionally, both values agreed reasonably, but in the majority of cases, they diverged widely. Interestingly, the samples SG-20, SG-23, and SG-26, obtained at the same carbonization temperature, did not show a decrease in the specific surface area with increasing particle size. This anomalous behavior can be explained on the basis of the particle form of SG-26. SG-20 and SG-23 formed more regular particles, of which the $500\text{ }\mu\text{m}$ particles exhibited $109\text{ m}^2\text{ g}^{-1}$ and the $595\text{ }\mu\text{m}$ particles exhibited $66\text{ m}^2\text{ g}^{-1}$. The SG-26 particles exhibited a basket-type form in which a concave curvature functioned as a convex surface of smaller size and contributed to an increase in the magnitude of the specific surface [7].

The SG-30 sample, by contrast, exhibited a type II isotherm (Fig. 1) with a hysteresis loop that was characteristic of solids with a mixture of tapered or wedge-shaped pores with open ends [25]. This observation suggested that at $600\text{ }^{\circ}\text{C}$, the porosity of the material increased. The results of pH_{pzc} showed that the carbon samples had surfaces with acidic to neutral characteristics.

3.2. Effects of pH on the UV–visible spectra of AO8

The spectra in Fig. 2a depict the principal visible band at 490 nm and a shoulder at 410 nm , demonstrating that AO8 was predomi-

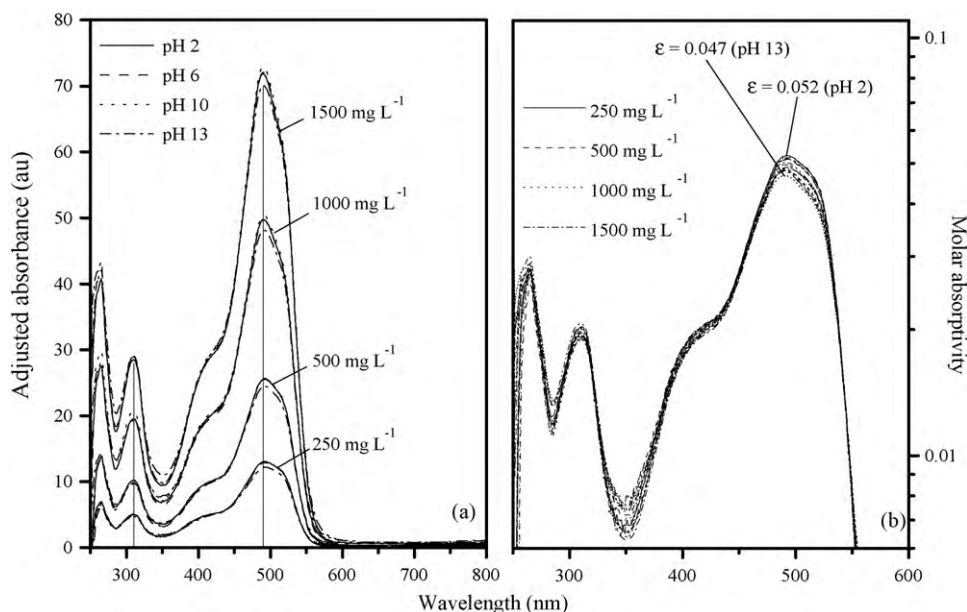


Fig. 2. Effect of the pH of dye solutions, at four concentrations, on the absorbance measurements. (a) Absorbance units and (b) molar absorptivity units.

nantly present in the hydrazone form rather than the azo form [19]. Given that pH was one of the parameters considered for optimization of the AO8 removal, the band positions as a function of pH were explored. The absence of bathochromic or hypsochromic shifts confirmed that the AO8 solutions were insensitive to pH changes due to the tautomer stability. This fact is important because shifts can produce errors in absorption measurements at the fixed initial wavelength of maximum absorbance. Moreover, the apparently light hypsochromic effect shown in Fig. 2b demonstrated a 10% difference between the molar absorptivity of the solutions at pH 2 and pH 13. Mostafa et al. [20] observed that the absorption of various sulfonic dyes in solution (including AO8) decreased upon addition of an electrolyte. Adjusting the solution pH by adding NaOH or HCl may disturb the water structure and can lead to association, aggregation, and, consequently, reductions in absorbance.

Little attention has been paid to the effects of pH on the absorbance bands of AO8. Any optimization study must account for factors that may reduce the accuracy of absorption measurements that indicate equilibrium concentrations. Arami et al. observed a slight shift in the wavelength of maximum absorbance of the azo dyes Direct Red 23 and Direct Red 80 as a function of pH [26]. Here, the effect of pH on the band intensity was found to be negligible. In an absorption study of the dye Reactive Black 5, Gibbs et al. [27] observed spectroscopic evidence for aggregation under certain experimental conditions: pH, dye concentration, and solution ionic strength. Ultimately, to avoid uncertainty in absorbance measurements due to dye removal under a given set of adsorption optimization conditions, a calibration curve for each pH value was measured and the following expressions were obtained: $A_{\text{pH } 2} = 1.1356 + 0.04753 C$ ($R^2 = 0.9992$); $A_{\text{pH } 6} = 1.6203 + 0.04805 C$ ($R^2 = 0.9994$); $A_{\text{pH } 10} = 1.3864 + 0.04805 C$ ($R^2 = 0.9993$); $A_{\text{pH } 13} = 0.7593 + 0.04654 C$ ($R^2 = 0.9995$).

3.3. Equilibrium study and adsorption isotherms

The kinetic experiments were performed at 20 °C using an initial AO8 concentration of 100 mg L⁻¹ with the carbon sample SG-26. Equilibrium was reached within 24 h (data not shown). Under the given conditions, the maximum adsorption capacity was 1 mg g⁻¹. The *pseudo*-first order kinetic constant calculated by the Lagergren model was $k_1 = 0.12 \text{ h}^{-1}$, the monolayer capacity a_m amounted 0.03 mg g⁻¹, and the correlation coefficient was $R^2 = 0.8957$. However, the kinetic rate was better described by Ho's *pseudo*-second order model [26]. The kinetic parameters were $k_2 = 2.34 \text{ g mg}^{-1} \text{ h}^{-1}$, $a_m = 1.05 \text{ mg g}^{-1}$, and $R^2 = 0.9864$.

As shown in Fig. 3, the adsorption isotherms were characteristic of the multilayer type-H4 isotherms of the Giles [28] classification system. The class H corresponds to adsorption of very large molecules and describes high adsorption affinities. The subgroup four is distinguished by a second rise and a second plateau. This behavior may be interpreted [28] either as adsorption at different surface regions or as re-orientation of the molecules on the adsorbed layer. Although the BET equation is principally appli-

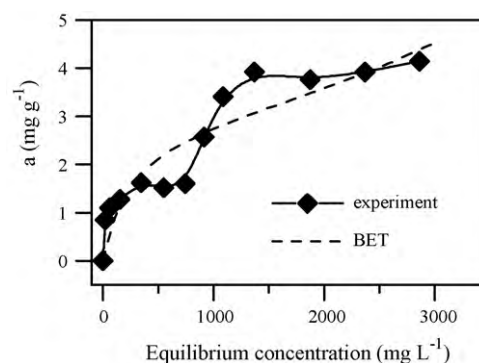


Fig. 3. Adsorption isotherm of AO8 on mesoporous carbon at 20 °C (continuous line). Experimental data and predicted BET isotherm (dashed line).

cable to solid–gas adsorption processes, we attempted to fit the experimental data to the multilayer adsorption from solution. The dashed line in Fig. 3 indicates that multilayer formation, via arrangement of a second monolayer on top of the first (BET consideration), did not occur. Most adsorption measurements for AO8 in an aqueous solution have shown monolayer behavior [5] within a concentration range spanned by our adsorption experiments. For instance, Karagad [29] reported the adsorption of AO8 on clinoptilolite with a maximum quantity of adsorbed dye of 44 mg g⁻¹. In contrast, a study of AO8 adsorption on mango seed carbon suggested formation of a monolayer with a capacity of 12 mg g⁻¹ using a 2000 mg L⁻¹ AO8 solution [5].

3.4. Determination of the optimal adsorption conditions

Using the orthogonal array L₁₆, with five factors and four levels, we performed a total of 32 trials (16 tests and their duplicates). A full factorial method was previously applied to an adsorption study that included 96 experiments in a 2-stage optimization procedure [30]. A fractional factorial design carried out 26 experiments (without duplication) for the adsorption of tanning dyes [13] using the same number of factors and levels. Indeed, fractional factorial experiments are more efficient than full factorial designs and yield better comparisons of individual factors. According to the Taguchi method, the percent of dye removal was selected as a response variable, and the experimental data were transformed into the $(S/N)_{\text{HB}}$ ratio. Results are listed in Table 2. The set mean $(S/N)_{\text{HB}}$ ratio for each level of the factors is summarized in Table 4. Fig. 4a shows the $(S/N)_{\text{HB}}$ response graph for the removal of AO8. The higher average $(S/N)_{\text{HB}}$ response represents the best level of each factor and was interpreted as the optimized removal efficiency. Therefore, the optimum treatment conditions were: temperature 10 °C, specific surface area 114 m² g⁻¹, initial concentration 500 mg L⁻¹, pH 2, and mass/volume ratio 150 g L⁻¹. This combination of factors and levels $A_1B_3C_2D_1E_4$ was not included in the 16 experiments of the orthogonal array. However, a confirmation experiment under these optimal conditions demonstrated 95% dye removal. If there is

Table 4

Average of the S/N response values obtained in the Taguchi analysis. $\bar{T} = 15.42$.

Factor	Mean $(S/N)_{\text{HB}}$ ratio				Analysis of variance		
	Level 1	Level 2	Level 3	Level 4	Degrees of freedom	Sum of squares	Variance
A	16.58	14.82	15.91	14.38	3	12.08	4.03
B	13.83	16.66	19.95	11.25	3	168.11	56.04
C	12.85	17.95	17.06	13.82	3	73.02	24.34
D	27.49	12.87	7.99	13.32	3	847.33	282.44
E	9.29	11.90	16.80	23.69	3	480.85	160.28
Error	–	–	–	–	0	–	–
Total	–	–	–	–	15	1581.39	–

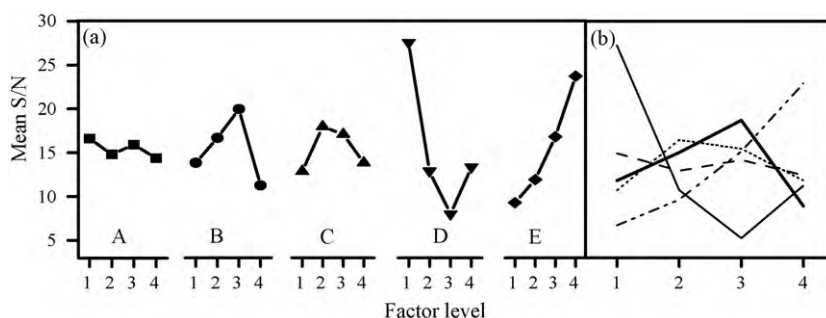


Fig. 4. Effect of each factor on the removal of AO8. (a) $(S/N)_{HB}$ graphical illustration of the response to each factor and (b) interaction between factors.

a match between the highest $(S/N)_{HB}$ values for a set of factors and the combination of experiments in the array, a verification experiment is unnecessary. An analysis of variance (ANOVA) was applied to detect any differences in the average performance of the transformed data, as shown in Table 4. The most influential factor was the pH (factor D) because the variance for this factor was the highest. In second place was the mass–volume ratio (factor E), a factor with significant variance. In agreement with the results reported by Karagad [29], the maximum removal of AO8 on a surfactant-modified zeolite was observed at lower pH values.

The effect of pH on the removal efficiency was analyzed in terms of the surface charge, as indicated by the pH_{pzc} values. The chemical groups on the carbon surface confer charges that influence the interaction between the solid and the ions in the solution. When the solution is acidic, $pH < pH_{pzc}$ (see Table 3), the total charge on the carbon surface will be positive. AO8 is an acidic dye containing a sulfonated group ($SO_3^- Na^+$) with a $pK_{a,1} = -0.2$ in the hydrazone tautomer form. Hence, higher adsorption of the dye may occur due to the increased electrostatic attraction between the negatively charged dye molecule and the positively charged carbon surface. The quantity of adsorbed dye at $pH > pH_{pzc}$ suggested a weaker interaction between the negative charge of the surface and the protonated $=NH^+ - NH-$ form and additionally, through van der Waals forces and hydrogen bonding in the adsorption process.

3.5. Prediction of other combinations by evaluating the estimate of the mean μ

The Taguchi method is a tool to predict combinations of experimental conditions that can yield good percentages of removal by adsorption. The procedure depends upon the additivity of the factorial effects. If the effect of one factor can be added to another to accurately predict the result, then good additivity exists. If an interaction between factors exists, then the additivity between those factors is poor. Interaction means that the effect of the first factor depends on the level of the second factor, and vice versa. Interactions between factors can be observed in Fig. 4b, in which a greater skew between the lines indicate a larger interaction strength. When the plotted lines are parallel or do not intersect, no interaction is present between the plotted factors. A factor effect at one specific level can be calculated using the mean $(S/N)_{HB}$ values (see Table 4) as well as the average of the entire experimental results, \bar{T} (all S/N values in Table 4). For instance, assume that the A_2B_2 treatment condition is to be estimated. Then $(\bar{A}_2 - \bar{T})$ represents the A_2 effect that changes the average from \bar{T} to \bar{A}_2 , and $(\bar{B}_2 - \bar{T})$ is the B_2 effect that changes the average from \bar{T} to \bar{B}_2 . The estimate of the mean is $\mu_{A_2B_2} = \bar{T} + (\bar{A}_2 - \bar{T}) + (\bar{B}_2 - \bar{T}) = \bar{A}_2 + \bar{B}_2 - \bar{T}$. The coefficient \bar{T} is one less than the items added to estimate the mean. To obtain the best estimate of the mean when an interaction is present, the effect of some factors can be grouped and averaged. In general, the less influential factors in different levels can be averaged. For example,

$\bar{A}_1\bar{B}_2$ indicates the average effect of factor A in level 1 and factor B in level 2, and the interaction (A_1B_2) is considered to be an item for the \bar{T} coefficient calculation.

Aside from the optimal conditions, we were interested in predicting other combinations that could yield good dye removal efficiency. Hence, an estimate of the mean of several combinations was calculated. The combinations with the highest mean were then selected. First, the $(S/N)_{HB}$ values of the factors D_1 (pH 2) and E_4 (m/v 150 $g L^{-1}$) were fixed because they were the most influential factors in the optimal level. The less influential factors (A, B, C) were averaged, and all possible 64 combinations of the levels of these factors were calculated. The expression used to estimate the mean was: $\mu_{A_iB_jC_kD_1E_4} = \bar{A}_i\bar{B}_j\bar{C}_k + \bar{D}_1 + \bar{E}_4 - 2\bar{T}$. The subscripts i, j , and k indicate the levels of the factors A, B, and C, which could be changed to yield different combinations. Because the average $\bar{A}_i\bar{B}_j\bar{C}_k$ is considered to be a single item, the coefficient of \bar{T} was 2. The four highest mean values were selected, and the experimental removal tests were conducted at the predicted combinations. The obtained percent dye removal values were higher than in any of the previous array experiments, as follows: 44% for the combination $A_3B_3C_2D_1E_4$, 74% for $A_3B_3C_3D_1E_4$, 82% for $A_2B_3C_2D_1E_4$, and 90% for $A_1B_3C_3D_1E_4$. In conclusion, this methodology was very helpful for achieving good removal efficiency with a minimal number of trials. Despite the usefulness of this Taguchi tool, no reports were found that described determination of the average of S/N for solute removal procedures.

3.6. Adsorption of real and simulated textile wastewater

As expected, the real wastewater contained high salt and organic contents, as judged from the high conductivity and COD values (a complete table is available in Supplement). Adsorption experiments were carried out using the real and simulated textile wastewater solutions (i) at the optimal conditions determined by the Taguchi results: 10 °C, 114 $m^2 g^{-1}$, pH 2, mass/volume ratio of 150 $g L^{-1}$, or (ii) at these conditions, except that the pH of the sample was left unchanged (pH of real wastewater 6, pH of simulated wastewater 13). The color removal of the wastewater samples was estimated from absorbance measurements at the wavelength of maximum absorbance: real wastewater, pH 2 and pH 6, at 561 nm; simulated wastewater, pH 2, at 490 nm; simulated wastewater, pH 13, at 319 nm. A shift in the wavelength of maximum absorbance was observed in the sample of simulated wastewater due to acidification. After adsorption at the optimal Taguchi conditions, the TOC and COD parameters did not decrease by more than 27% due to the high organic load in the initial wastewater. However, the color intensity decreased to 78% of the value of the original wastewater, to 56% for the acidified wastewater, and to 76%, both at pH 2 and pH 6, of the original simulated wastewater, which contained a mixture of acidic, basic, and natural dyes.

4. Conclusions

The use of guava seeds as an activated carbon precursor presents an alternative purification substrate for the removal of AO8 from aqueous solutions. The Taguchi method was suitable for optimizing the adsorption parameters; several factors could be studied simultaneously with a minimal number of trials. Because the number of possible combinations of five factors with four levels each was 1024, the Taguchi methodology, which prescribed testing 16 combinations, was a valuable strategy. The initial pH was shown to yield the largest effect on dye removal efficiency; in particular, lower pH values favored the removal of AO8. Surprisingly, the specific surface area was not the most influential factor, as in most previous adsorption studies. In this case, the dye removal was dominated by the physical forces as well as the ionic interactions between the surface and the ionic dye. The proposed methodology demonstrates that pollutant removal can be optimized for application to real wastewater.

Acknowledgements

EGD thanks the grant (168847) received from CONACyT and authors acknowledge the support of the project CB-2008-01-100439 from the same organization.

Appendix A. Supplementary data

Supplementary data associated with this article can be found, in the online version, at doi:10.1016/j.cej.2010.07.040.

References

- [1] C. O'Neill, F.R. Hawkes, D.L. Hawkes, N.D. Lourenço, H.M. Pinheiro, W. Deleé, Colour in textile effluents – sources, measurement, discharge consents and simulation: a review, *J. Chem. Technol. Biotechnol.* 74 (1999) 1009–1018.
- [2] P. Gregory, Toxicology of textile dyes, in: R.M. Christie (Ed.), *Environmental Aspects of Textile Dyeing*, Woodhead Publishing Textiles, 2007, pp. 44–72.
- [3] H. Metivier-Pignon, C. Faur-Brasquet, P. Le Cloirec, Adsorption of dyes onto activated carbon cloth: approach of adsorption mechanisms and coupling of ACC with ultrafiltration to treat coloured wastewaters, *Sep. Purif. Technol.* 31 (2003) 3–11.
- [4] H. Metivier-Pignon, C. Faur, P. Le Cloirec, Adsorption of dyes onto activated carbon cloth: using QSPRs as tools to approach adsorption mechanisms, *Chemosphere* 66 (2007) 887–893.
- [5] M.M. Dávila-Jiménez, M.P. Elizalde-González, V. Hernández-Montoya, Performance of mango seed adsorbents in the adsorption of anthraquinone and azo acid dyes in single and binary aqueous solutions, *Bioresour. Technol.* 100 (2009) 6199–6206.
- [6] M.P. Elizalde-González, V. Hernández-Montoya, Guava seed as an adsorbent and as a precursor of carbon for the adsorption of acid dyes, *Bioresour. Technol.* 100 (2009) 2111–2117.
- [7] M.P. Elizalde-González, V. Hernández-Montoya, Removal of acid orange 7 by guava seed carbon: a four parameter optimization study, *J. Hazard. Mater.* 168 (2009) 515–522.
- [8] C.I. Guaratini, M.V.B. Zaroni, Corantes Têxteis, *Quimica Nova* 23 (2000) 71–78.
- [9] K. Hunger, *Industrial dyes: Chemistry, Properties, Applications*, Wiley-VCH, Germany, 2003.
- [10] O.J. Hao, H. Kim, P.C. Chiang, Decolorization of wastewater, *Crit. Rev. Sci. Technol.* 30 (2000) 449–505.
- [11] R. Loos, G. Hanke, S.J. Eisenreich, Multi-component analysis of polar water pollutants using sequential solid-phase extraction followed by LC-ESI-MS, *J. Environ. Monit.* 5 (2003) 384–394.
- [12] C.E. Clarke, F. Kielar, H.M. Talbot, K.L. Johnson, Oxidative decolorization of azo dyes by a Mn oxide containing waste, *Environ. Sci. Technol.* 44 (2010) 1116–1122.
- [13] V. Gómez, M.P. Callao, Modeling the adsorption of dyes onto activated carbon by using experimental design, *Talanta* 77 (2008) 84–89.
- [14] N. Daneshvar, A.R. Khataee, M.H. Rasoulifard, M. Pourhassan, Biodegradation of dye solution containing malachite green: optimization of effective parameters using Taguchi method, *J. Hazard. Mater.* 143 (2007) 214–219.
- [15] P. Ross, *Taguchi Techniques for Quality Engineering*, Mc Graw-Hill International Editions, Singapore, 1996.
- [16] M.P. Elizalde-González, V. Hernández-Montoya, Fruit seeds as adsorbents and precursors of carbons for the removal of anthraquinone dyes, *Int. J. Chem. Eng.* 1 (2008) 145–155.
- [17] R. Devi, V. Singh, A. Kumar, COD and BOD reduction from coffee processing wastewater using Avacado peel carbon, *Bioresour. Technol.* 99 (2008) 1853–1860.
- [18] P. Klobes, K. Meyer, R.G. Munro, Porosity and Specific Surface Area Measurements for Solid Materials, national Institute of Standards and Technology, Washington, 2006.
- [19] A.S. Özen, V. Aviyente, G. Tezcanli-Güyer, N.H. Ince, Experimental and modeling approach to decolorization of azo dyes by ultrasound: degradation of the hydrazone tautomer, *J. Phys. Chem. A.* 109 (2005) 3506–3516.
- [20] O.I. Mostafa, S.A. Abo Farha, M.M. El-Fass, Aggregation and tautomeric properties of some acid dyes. Part II, *Afinidad* 62 (2005) 137–143.
- [21] Waste Water Ordinance – AbwV of 17, Federal Ministry for the Environment, Nature Conservation and Nuclear Safety, Germany, June 2004.
- [22] O. Ozdemir, M. Turan, A.Z. Turan, A. Faki, A.B. Engin, Feasibility analysis of color removal from textile dyeing wastewater in a fixed-bed column system by surfactant-modified zeolite (SMZ), *J. Hazard. Mater.* 166 (2009) 647–654.
- [23] S.J. Gregg, K.S.W. Sing, *Adsorption, Surface Area and Porosity*, Academic Press, New York, 1982.
- [24] P.C.C. Faria, J.J.M. Órfão, M.F.R. Pereira, Adsorption of anionic and cationic dyes on activated carbons with different surface chemistries, *Water Res.* 38 (2004) 2043–2052.
- [25] S. Lowell, J.E. Shields, M.A. Thomas, M. Thommes, *Characterization of Porous Solids and Powders: Surface Area, Pore Size and Pensity*, Springer, Netherlands, 2006.
- [26] M. Arami, N.Y. Limaee, N.M. Mahmoodi, N.S. Tabrizi, Removal of dyes from colored textile wastewater by orange peel adsorbent: equilibrium and kinetics studies, *J. Colloid Interf. Sci.* 288 (2005) 371–376.
- [27] G. Gibbs, J.M. Tobin, E. Guibal, Influence of chitosan preprotonation on reactive black 5 sorption isotherms and kinetics, *Ind. Eng. Chem. Res.* 43 (2004) 1–11.
- [28] C.H. Giles, T.H. MacEwan, S.N. Nakwa, D. Smith, Studies in adsorption. Part XI. A system of classification of solution adsorption isotherms, and its use in diagnosis of adsorption mechanisms and in measurement of specific surface areas of solids, *J. Chem. Soc.* 3 (1960) 3973–3993.
- [29] D. Karagad, Modeling the mechanism, equilibrium and kinetics for the adsorption of acid orange 8 onto surfactant-modified clinoptilolite: the application of nonlinear regression analysis, *Dyes Pigments* 74 (2007) 659–664.
- [30] L.C. Morais, O.M. Freitas, E.P. Goncalves, L.T. Vasconcelos, G.C. González Beça, Reactive dyes removal from wastewaters by adsorption on eucalyptus bark: variables that define the process, *Water Res.* 33 (1999) 979–988.